DYNAMIC MODELLING OF PROTON EXCHANGE MEMBRANE FUEL CELLS FOR ELECTRIC VEHICLE APPLICATIONS

A. A. Abd El Monem[1], Ahmed M. Azmy[2], S. A. Mahmoud[3]

[1] *Electric Senior Engineer, Khalda Petroleum Company, Egypt*

[2] Head of *Elec. Power and Machines Engineering Department, Faculty of Engineering, Tanta University, Egypt*

[3] *Electrical Engineering Department, Faculty of Engineering, Menoufiya University, Shebin El-Kom, Egypt*

ABSTRACT

This paper presents a simplified mathematical model for proton exchange membrane fuel cell (PEMFC) systems. The system performance is validated through a comparison with experimental datasheet results of a commercial PEMFC stack. The model is then used to study the transient response of a PEMFC when subjected to different load variations. A PI controller is designed to control the fuel cell output voltage during different transient conditions. The results ensure that the model provides an accurate representation of the dynamic and steady state behaviour of the fuel cell. In addition, the results show the fast response capabilities of the PEMFC for following changes in the load. This model will be useful for the optimal design and real-time control of PEMFC systems especially for electric vehicles applications.

يقدم هذا البحث نموذجاً رياضياً مبسطاً لأنظمة خلايا الوقود ذات غشاء تبادل البروتونات. وقد تم التحقق من أداء هذا النظام عن طريق مقارنته مع نتائج اختبارية لخلية وقود تجارية ذات غشاء تبادل البروتونات. بعد ذلك استُخدم هذا النموذج لدراسة الاستجابة العابرة لخلية وقود ذات غشاء تبادل البروتونات عند تعرضها لتغييرات مختلفة في الأحمال. وللتحكم في جهد الخرج لخلية الوقود أثناء الحالات العابرة فقد تم تصميم حاكم تناسبي تكاملي. وقد أكدت النتائج أن هذا النموذج يعطي تمثيلاً حقيقياً للسلوك العابر والسلوك الساكن لخلية الوقود. بالاضافة الى ذلك أظهرت النتائج مقدرة خلية الوقود ذات غشاء تبادل البروتونات علي الاستجابة السريعة للتغيرات في الحمل. وللاستفادة من هذا النموذج يمكن استخدامه في التصميم المثالي والتحكم التزامني لأنظمة خلايا الوقود ذات غشاء تبادل البروتونات و بالأخص فيما يتعلق بتطبيقات المركبات الكهربية.

Index Terms- Brushless doubly-fed machine- Dynamic modelling- Generalized theory- Induction ma chine- Self-cascaded, Speed control- Variable speed drives

NOMENCLATURE

A	Tafel slope
C_S	Surface concentration
C_B	Bulk concentration
E	Ideal fuel cell potential (in volts)
E_{theor}	Reference potential (in volts)
$E^o_{theor.actual}$	Actual theoretical voltage (in volts)
E^o_{theor}	Ideal standard potential at 298K (in volts)
E_{losses}	Loss voltage (in volts)
E_n	Nernst voltage (in volts)
E_{oc}	Open circuit voltage (in volts)
F	Faraday constant (96485 coulombs per mole)
H	Planck constant (6.626×10^{-34} J.s)
i_o	Exchange current (in amps)
i_{fc}	Fuel cell current (in amps)
$I_{\lim it}$	Limitation current (in amps)
K	Boltzmann constant (1.38×10^{-23} J/K)
K_E	Empirical constant in calculating $E^0_{theor.actual}$ (in volt per Kelvin)
K_r	Modelling constant
N	Number of cells in the stack
n	Number of electrons participating in the reaction
P_{air}	Absolute supply pressure of air (atm)
P_{fuel}	Absolute supply pressure of fuel (atm)
P_{H2}	Partial pressure of hydrogen inside the stack
P_{O2}	Partial pressure of oxygen inside the stack
R	Gas constant, 8.3145 J/ (mol.K)
T	Temperature of operation (in Kelvin)
U_f	Utilization factor (%)
U_{fH2}	Rate of conversion (utilization) of hydrogen (%)
U_{fO2}	Rate of conversion (utilization) of oxygen (%)
$V_{lpm(air)}$	Air flow rate (l/min)
$V_{lpm(fuel)}$	Fuel flow rate (l/min)
V_{cell}	Cell voltage (in volts)
V_{act}	Activation voltage (in volts)
V_{conc}	Concentration voltage (in volts)
V_{ohm}	Ohmic voltage (in volts)
V_{out}	Output voltage of fuel cell stack (in volts)
W_{el}	Maximum electrical work of fuel cell (Joules)
x%	Percentage of hydrogen in the fuel (%)
y%	Percentage of oxygen in the air (%)
z	Number of moving electrons
α	Charge transfer coefficient
ΔG	Change in Gibbs free energy (Joules per mole)
ΔG^0	Gibbs free energy change of reaction at the standard state (pressure 1 atm and temperature 298 K)
ΔH	Enthalpy change
ΔS	Entropy change

1. INTRODUCTION

Fossil fuel represents a major source of the global environmental problems, particularly the global warming and destruction of ozone. A major utilization of fossil fuel is the transportation sector [1]. Thus, it is urgently required to eliminate or reduce the pollution from transportation systems.

Fuel cells can play this role since they represent one of the most promising sources of renewable energy. They are considered as clean sources with extremely low emission of oxides, nitrogen and sulphur. In addition, they are advantageous by high generation efficiency, very low noises and fuel flexibility [2]. Fuel cells can utilize hydrogen directly to produces dc power [2], which can be used to power vehicles, electronic devices, houses or the main grid system [3]. The absence of intermediate conversion, mechanical and combustion process gives many additional advantages for the fuel cells [4].

The commonly used fuel cells can be classified according to temperature into: low, medium, and high-temperature fuel cells. Low-temperature units include alkaline fuel cell (AFC) and proton exchange membrane fuel cell (PEMFC). Phosphoric acid fuel cell (PAFC) represents a medium-temperature unit, while high-temperature fuel cells include molten carbonate fuel cells (MCFC) and solid oxide fuel cells (SOFC) [5].

PEMFCs are appointed for vehicle applications due to their high power density, low operating temperature, i.e. fast start-up, good dynamic behaviour, simple and compact design, reliable operation, and non-corrosive electrolyte [2]. The ordinary operation of electric vehicle necessitates repetitive cycles of start, stop, acceleration and deceleration, which represents continuous transient situations [6].

The development of fuel cells for electric vehicle applications requires simulating the dynamic behaviour of the entire system. The fast response of the system and the real-time accurate simulations have also to be considered. These requirements are necessary to support the real design and implementation of fuel cells in vehicle applications. Also, system behaviour can be studied by means of

computer simulations under different loading conditions, pressure of reagent gases and temperature [7].

Several mathematical models have been presented to describe the behaviour of PEM fuel cells [8]-[13]. Most of them provided the simulation only for the steady-state behaviour [8], [9]. In practical applications of electric vehicle fields, the output power of the fuel cell experiences significant variations mainly during acceleration and deceleration. During these situations, steady-state models will not be sufficient to represent the transient dynamics and hence, the analysis of their dynamic performance will be unrealistic.

Many of the previously-introduced dynamic models are complex since they depend on several partial differential equations [10], [11]. This complexity is undesirable since it results in large simulation time especially when the fuel cell is interfaced with other systems, such as electric vehicles

Dynamic models reported in [12], [13] did not take the double layer charging effect into account. The regions where mass transfer limitations occur have not been considered in the dynamic models presented in [13].

In recent years, fuel cells for electric vehicle applications are rapidly increased. This paper proposes a simplified but accurate mathematical model for PEM fuel cell systems. A suitable PI controller is designed to control the fuel cell output voltage. Both the double layer charging effect and the thermodynamic characteristic inside the fuel cell are included in the model.

The model simulation results obtained at steady state are validated by comparing them with datasheet results provided by the manufacturer [14]. In addition, the dynamic performance is studied under some disturbances. The model is implemented using the simulation environment MATLAB/SIMULINK

2. DYNAMIC MODELLING OF PEMFCs

A simplified dynamic model of a fuel cell with proton exchange membrane (PEM) type, based on physical-chemical knowledge of the phenomena occurring inside the fuel cell is presented in this section. To simplify the analysis, the following assumptions are made [15]:
1- One-dimensional treatment, i.e. all quantities vary only in an orthogonal direction to anode and cathode surfaces
2- Ideal and uniform distribution of gases
3- Constant pressures in the gas flow channels of the unit
4- Humidified hydrogen and air are used as fuel and oxidant respectively

5- The operating temperature is 100 °C and the reaction products are in a liquid state
6- The average stack temperature is considered when evaluating the thermodynamic properties, where temperature variations across the stack are neglected, and only the average specific heat capacity of the stack is used
7- Parameters of the fuel-cell stack are obtained by augmenting parameters of individual cells

For understanding the operation of fuel cells, the ideal performance is firstly defined. Then, losses arising from non-ideal behaviour can be estimated and then deducted from the ideal performance to investigate the actual operation.

3.1 The Gibbs Free-Energy and Nernst Potential

When the fuel cell operates at constant temperature and pressure, the maximum electrical work (W_{el}) that can be obtained is given by the change in Gibbs free energy (ΔG) of the electrochemical reaction as follows [16]:

$$W_{el} = \Delta G = -n \times F \times E_{theor}$$

(1)

where: "n" is the number of electrons participating in the reaction, "F" is the Faraday constant (96485 coulombs per mol), and "E_{theor}" is the reference potential (in volts)

The Gibbs free-energy change can be calculated as follows [4]:

$$\Delta G = \Delta H - T\,\Delta S \qquad\qquad (2)$$

where: "ΔH" is the enthalpy change and "ΔS" is the entropy change.

"ΔH" represents the total thermal energy; while the enthalpy change minus the quantity "$T\Delta S$" represents the available free energy. "$T\,\Delta S$" is the amount of heat produced by the fuel cell operating reversibly, with "T" is the operating temperature in Kelvin. The electrochemical oxidation and reduction reactions in a hydrogen/oxygen (H_2/O_2) fuel cell are given by following reactions:

Anode reaction: $\quad H_2 \longrightarrow 2H^+ + 2e^-$

(3)

Cathode reaction: $\quad \dfrac{1}{2}O_2 + 2H^+ + 2e^- \longrightarrow H_2O$

(4)

The overall reaction: $H_2 + \dfrac{1}{2}O_2 \longrightarrow H_2O$
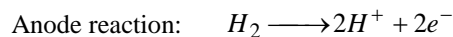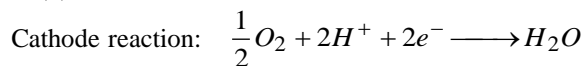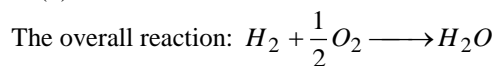
(5)

For every mole of hydrogen consumption, the cell consumes 0.5 mole of oxygen and produces one mole of water. In addition, two moles of electrons are produced. The Gibbs free energy change of reaction is given by the following equation [16]:

$$\Delta G = \Delta G^0 - R \times T \ln(P_{H2})(P_{O2})^{1/2}$$
$$(6)$$

where: "ΔG^0" is the Gibbs free energy change of reaction under standard conditions (pressure = 1 atm and temperature = 298 K), "R" is the gas constant, 8.3145 J/ (mol.K), "P_{H2}" is the partial pressure of hydrogen inside the stack and "P_{O2}" is the partial pressure of oxygen inside the stack.

The theoretical potential (E_{theor}^0) for the H_2/O_2 cell reaction is derived from the change in the Gibbs free energy (ΔG^0) as follows [4]:

$$E_{theor}^0 = -(\frac{\Delta G^0}{z \times F})$$
$$(7)$$

where: "z" is the number of moving electrons.

From equations (1), (6) and (7), the general form of the Nernst equation is obtained as follows [5], [12], [17]:

$$E_n = E_{theor} = E_{theor.actual}^0 + \frac{RT}{zF} \ln(P_{H2})(P_{O2})^{1/2}$$
$$(8)$$

where: "$E_{theor.actual}^0$" is a function of temperature and can be expressed as:

$$E_{theor.actual}^0 = E_{theor}^0 - K_E(T-298)$$
$$(9)$$

where: "K_E" is the empirical constant for calculating $E_{theor.actual}^0$ (volt per Kelvin)

3.2 Ideal Performance

In equation (8), E_{theor} gives the ideal open circuit cell potential. This potential defines the maximum performance that can be obtained from a fuel cell. The Nernst equation is used to relate the ideal standard potential (E_{theor}^O) and the ideal equilibrium potential (E_{theor}) at other partial pressures of reactants. Generally, the cell potential increases with the increase of partial pressure (concentration) of reactants and a decrease in the partial pressure of products. Thus, the ideal potential can be increased by increasing the reactant pressures at a given temperature and hence, higher pressures cause improvements in fuel cell performance [18].

The ideal potential (E_{theor}^O) at 298 K and with pure hydrogen and oxygen is 1.229 volts with liquid water product, and 1.18 volts with gaseous water product. This value is sometimes referred to as the oxidation potential of hydrogen [19]. The difference between the two volts, i.e. 1.229 volts and 1.18 volts, is the Gibbs free energy change of water vaporization under standard conditions [4].

The reactant concentrations affect open circuit voltage of a fuel cell, where maximum ideal potential takes place when the reactants at the anode and cathode are pure. For fuel cells that utilize air and/or impure dry hydrogen, the potential will be decreased. In addition, the decrease of reactants concentration at the exit of the cell compared to at the entrance causes a Nernst correction that reduces the open circuit voltage. To obtain the best performance for low-temperature fuel cells, such as PEM fuel cell, a noble metal electro-catalyst, such as platinum (Pt) has to be used [4], [18].

3.3 Actual Performance

A. Polarization Characteristics of PEM Fuel Cells

The electrochemical process within fuel cells is associated with many losses as shown in figure 1 [20]. The reasons of these losses are: activation polarization, Ohmic polarization, and concentration polarization. Due to these losses, the cell voltage (V) is less than the ideal value "E" as follows:

$$V = E - E_{losses} \qquad (10)$$
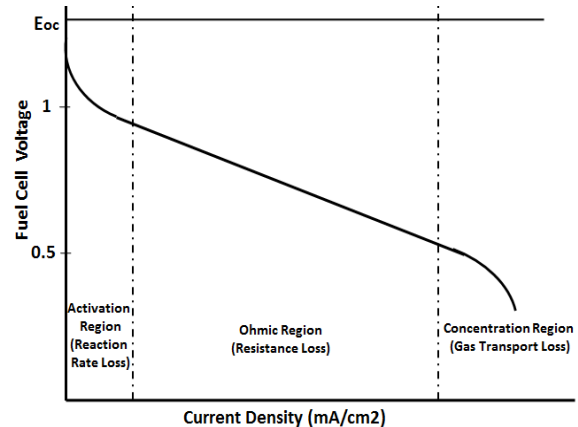
Fig. 1. Ideal and actual voltage/current characteristic of PEM fuel cell

The activation polarization loss appears mainly at low currents, where there is a need to overcome the electronic barriers before current and ion flow. Ohmic polarization loss, in contrast, is almost proportional to current, and it increases with the current since cell resistance is almost constant. Finally, the gas transport losses take place commonly at high limiting currents. The reason is the difficulty of providing sufficient reactants flow to the cell reaction sites. However, this kind of losses occurs also over the entire range of current, but with lower effect [20].

● *Activation loss:*

The main reason of activation loss is the slowness of the reactions at the electrode surfaces. To force the electrons to the electrodes through the chemical reaction, a portion of the potential is lost. The Tafel equation is commonly used to account for these

losses [19]. Using this equation, a relation between the overvoltage at the electrode surface and the natural logarithm of current density can be derived. Thus, the activation voltage loss for the fuel cell can be obtained as follows [17]:

$$V_{act} = -A \ln i_{fc}$$

(11)

$$A = \frac{RT}{z\alpha F}$$

(12)

where: "i_{fc}" is the fuel cell current in Ampere, "A" is the Tafel slope and "α" is the charge transfer coefficient, which depends on the type of electrodes and catalysts used.

● *Ohmic loss:*

The ohmic resistance of a PEM fuel cell consists of three terms: the resistance of polymer membrane, the conducting resistance between the membrane and electrodes, and that of electrodes. The total ohmic voltage drop can be expressed as follows [17]:

$$V_{ohm} = V_{ohm,a} + V_{ohm,membrane} + V_{ohm,c} = I_{fc} R_{ohm}$$

(13)

● *Concentration loss:*

As a result of mass diffusions from the flow channels to the reaction sites, concentration gradients can be formed during the reaction process. The reason of concentration voltage drop at high current densities is the slow transportation of reactants to the reaction sites. It is also possible that the catalyst surfaces at the anode and cathode are covered by a water film. The concentration over potential can be written as follows [17]:

$$V_{conc} = -\frac{R \times T}{z \times F} \ln \frac{C_S}{C_B}$$

(14)

Where: "C_S" and "C_B" are the surface and bulk concentrations respectively.

The above equation can be rewritten as [17]:

$$V_{conc} = -\frac{R \times T}{z \times F} \ln(1 - \frac{I_{fc}}{I_{\lim it}})$$

(15)

where: "$I_{\lim it}$" is the limitation current (A)

Finally, the equivalent concentration resistance is:

$$R_{conc} = \frac{V_{conc}}{I_{fc}} = -\frac{R \times T}{z \times F \times I_{fc}} \ln(1 - \frac{I_{fc}}{I_{\lim it}})$$

(16)

B. Dynamics of PEMFCs

● *Double-Layer Charging Effect*

Any collection of charges, e.g. hydrogen ions (in the electrolyte) and electrons (in the electrodes), will generate an electrical voltage. When this layer of charges is formed at the surface of electrode and electrolyte, it will represent a store of electrical charges similar to a capacitor. With the current changes, the charge will change during a certain time

and hence, the voltage will not immediately follow the current changes unlike the ohmic voltage drop. This results in an instant voltage change after any current change owing to the internal resistance and then the voltage will change gradually to its final value. Considering the effect of the double layer while building the PEM fuel cell dynamic model will give the model more accuracy when describing the dynamic performance. Thus, it is quite reasonable to use a capacitor to model the capacitance effect resulting from the charge double layer [7], [15].

● *Flow rate and thermodynamics characteristics:*

There are delays between the change in the load current and flow rates of fuel and air which represented in this model by using inductance. Another delay is used to represent thermodynamics time constant inside the fuel cell. Thus, the fuel cell fuel and oxidant flow delays, the thermodynamic characteristics and the double layer effects will dominate the transient responses of the fuel cell model.

C. Cell Voltage

The open-circuit voltage can be calculated as follows [21]:

$$E_{oc} = N \times E_n \qquad (17)$$

where: "E_{oc}" is actually the open-circuit voltage of the fuel cell. However, under normal operating conditions, the fuel cell output voltage is less than E_{oc}. Taking into consideration the activation loss, ohmic resistance voltage drop, and concentration over potential, the cell voltage is given as [21]:

$$V_{cell} = E_{oc(cell)} - V_{act(cell)} - V_{ohm(cell)} - V_{conc(cell)}$$

(18)

To represent a fuel-cell stack, the parameters of individual cell are lumped and the output voltage of the fuel cell is obtained as [16], [17]:

$$V_{out} = N \times V_{cell} = E_{oc} - V_{act} - V_{ohm} - V_{conc}$$

(19)

D. Reactant Utilization

Reactant utilization has a major impact on fuel cell performance. A utilization factor "U_f" is defined to represent the ratio of the amount of hydrogen that reacts with the oxygen to the amount of hydrogen entering the anode. The rate of conversion (utilization) of hydrogen "U_{fH2}" and oxygen "U_{fO2}" are determined as follows [22]:

$$U_{fH2} = \frac{K_r RTNi_{fc}}{zFP_{fuel}V_{lpm(fuel)}x\%} , \quad 0 \le U_{fH2} \le 1$$

(20)

$$U_{fO2} = \frac{K_r \times R \times T \times N \times i_{fc}}{2\, z\, F\, P_{air}\, V_{lpm(air)}\, y\%}, \qquad 0 \leq U_{fO2} \leq 1$$

(21)

Where: "K_r" is the modelling constant, "N" is the number of cells in the stack, "P_{fuel}" is the absolute supply pressure of fuel (atm), "$V_{lpm(fuel)}$" is the fuel flow rate (l/min), "$x\%$" is the percentage of hydrogen in the fuel (%), "P_{air}" is the absolute supply pressure of air (atm), "$V_{lpm(air)}$" is the air flow rate (l/min) and "$y\%$" is the percentage of oxygen in the air (%).

The partial pressures P_{H2} and P_{O2} are determined as follows [22]:

$$P_{H2} = P_{Fuel} \times x\% \times (1 - U_{fH2})$$

(22)

$$P_{O2} = P_{Air} \times y\% \times (1 - U_{fO2})$$

(23)

The exchange current is given as follows [23], [24]:

$$i_o = \frac{z \times F \times k(P_{H2} + P_{O2})}{R \times h} e^{\frac{\Delta G}{R \times T}}$$

(24)

where: "K" is the Boltzmann constant, 1.38×10^{-23} J/K and "h" is the Planck constant, 6.626×10^{-34} J.s

The complete model of the fuel cell is built based on the abovementioned equations as shown in Figure 2. The figure indicates the logical connections of the different blocks and shows the different inputs and outputs.
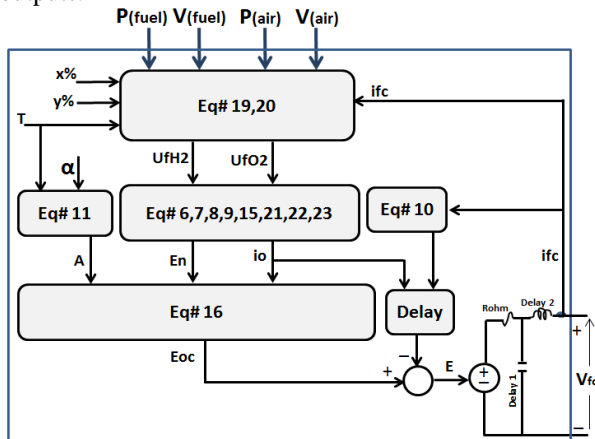
Fig. 2. The general diagram model of PEMFCs

The model is simulated by MATLAB/SIMULINK using the available data sheet of NedStack PS6 fuel cell, 6kW [20]. For electric vehicle applications, the fuel cell model should be rescaled to be suitable for the electric vehicle power demand. Figure 3 shows the block diagram of MATLAB/SIMULINK model, which has been developed for the PEMFC.
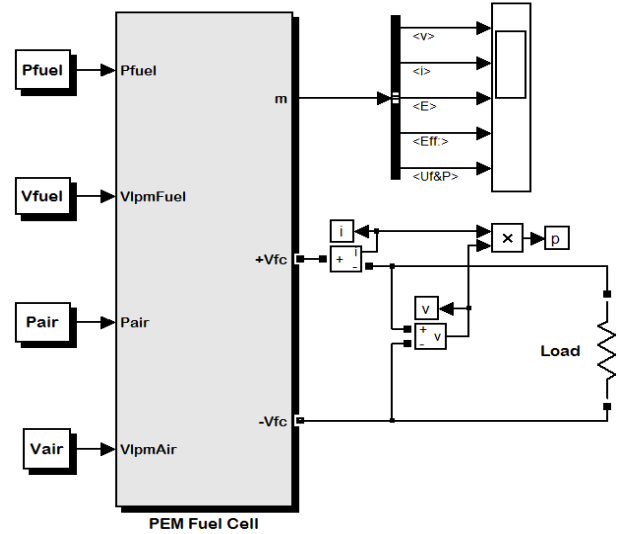
Fig 3. The block diagram of MATLAB/SIMULINK model of PEMFCs

3. MODEL VALIDATION

4.1 Simulation and Datasheet Data

The results for base case operating conditions were verified by comparing them with datasheet results provided by the manufacturer [14]. The comparison is given in Figure 4.
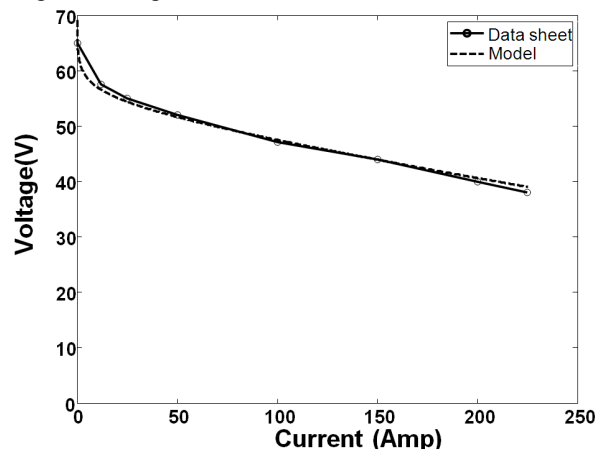
Fig. 4. Polarization curves of the fuel cell according to the proposed model and the datasheet

The polarization curve of the cell potential versus the cell current for the model is in a good agreement with the datasheet polarization curve in the intermediate load region. However, there are minor differences between the model and datasheet results in low load region and mass transport limitation region. The difference in the low load region or the activation region is due to the estimation of some parameters affecting the activation regions, which are not available in the datasheet. For the difference in the mass transport limitation region, the curve obtained from the model is shifted upward compared

to the datasheet results. However, this difference is acceptable taking into account neglecting some physical process such as water flooding at the cathode and anode drying.

Another verification process is the comparison of the model and datasheet power curves, which is shown in Figure 5. Similar to the polarization curve, the model power curve is very close to the datasheet curve in the load region below the mass transport region. At high loading condition in Figure 5, the predicted values are slightly higher than the datasheet values as can be expected for the same abovementioned reasons.

From these comparisons, it is clear that the developed model has a high accuracy and can be used to simulate the performance of the fuel cell unit.
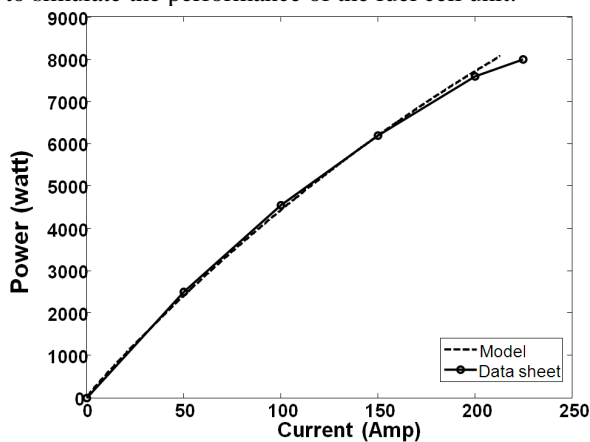
Fig. 5. Power-current curves according to the model and datasheet

4.2 Load variation Study

The load is modelled as a constant power load using the three-phase load block that can be set by defining the required power. The dynamic performance of the fuel cell model is investigated under different load variations, using step increase and decrease changes in the load. A PI controller is designed and tuned to control the output fuel cell voltage during transient operation by varying the flow rates of fuel and air.

FC output voltage, current and power are selected to study the dynamic performance of the PEMFC developed model. After the FC starts and reaches the steady state values of voltage and current, a step change is applied. Figure 6 shows MATLAB/SIMULINK model with a PI controller, which has been developed for the PEMFC. All results shown in figures 7, 8 and 9 are obtained using the PI controller. In addition, the output voltages of the unit without PI controller are shown in the same figures with the dotted lines.
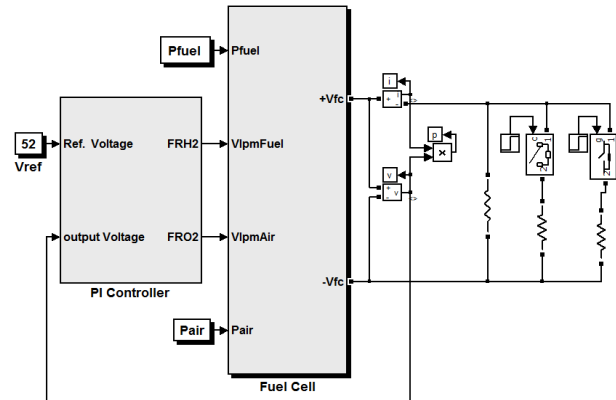
Fig. 6. MATLAB/SIMULINK model with PI controller

● *Case 1- Load increase:*

As shown in Figure 7, the FC started with a load of 2 kW, where the PI controller regulates the output voltage within 6 sec to reach 52 volt, the reference value, at steady state by adjusting the fuel and airflow rates. A step load increase with 300 W is applied after 30 sec.
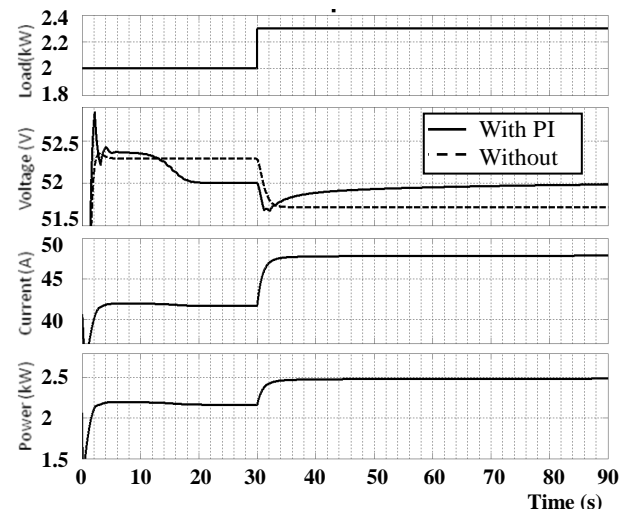
Fig. 7. Results of step load increase

From the results, it is evident that the current increases as a result of the load increase but with a certain delay. Consequently, the output voltage of the fuel cell decreases with a time delay due to the flow rates of fuel and air. Generally, the shown time delay following the load power change is due to the fuel-cell time constant. The PI controller showed a good and relatively fast response in controlling the output voltage after the starting and the load increase. Thus, through the regulation of the fuel and airflow rates, the PI controller succeeded to keep the voltage at the 52 V level according to the reference value.

Case 2- Load decrease:

In this case, the FC is loaded with 2 kW and a step load decrease of 200 W is applied at a time of 30 sec. The results are shown in Figure 8, where the decrease in the load causes a decrease in the current with a

time delay. The output voltage of the unit increases as a result of the voltage-drop decrease with a time delay due to flow rates of fuel and air. Once again, the PI controller succeeded to regulate the output voltage and maintain its level at the reference value. Without controller, the voltage reaches the 52V level after the load change and faster than with the controller. However, it is not always the case under different loading conditions, e.g. with a load of 1.9 kW. Thus, the controller ensures maintaining the voltage at its desired value under all loading conditions.
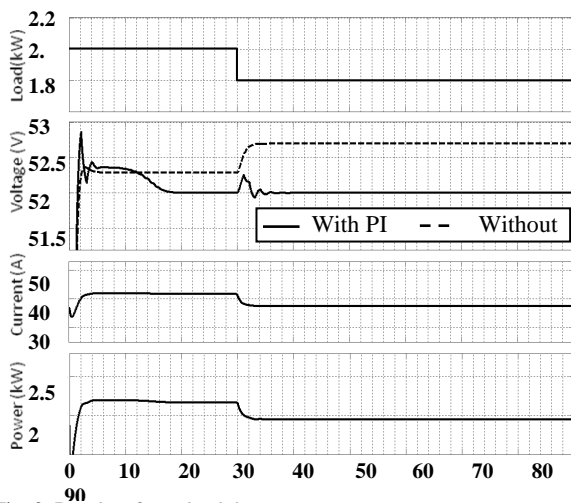
Fig. 8. Results of step load decrease

Case 3- Load increase and decrease:

The third case represents a composite disturbance, where two sequential disturbances are applied. Firstly, a step load increase is applied at 15 sec from 1950 W to 2350 W, and then a step load decrease is applied at 85 sec from 2350 W to 1900 W as shown in Figure 9. It is clear that the PI controller is able to control the output voltage in a proper time. This indicates that the controller performs well even starting from different initial operating points.

4. INTENDED EXTENSION WORK

It is intended to implement the developed verified dynamic model to an electric vehicle system. The target is to enhance the transient performance of the vehicle through a control design of the firing angles of the Fuel Cell converter and the electric motor as shown in Figure 10. In an ongoing research, the model of the overall vehicle system including the PEM fuel cell will be introduced. In addition, suitable controllers will be developed in detail and the performance of the system will be discussed.
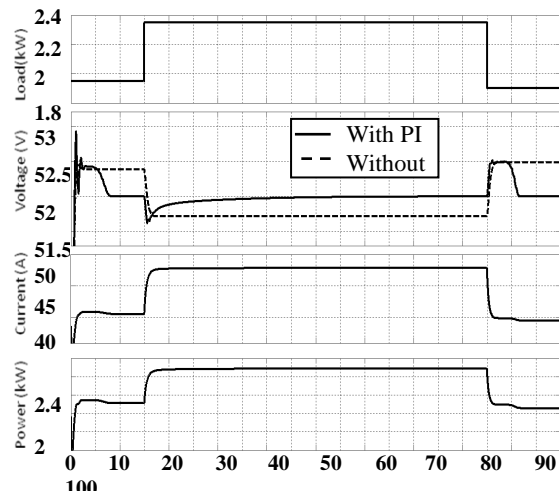
Fig. 9. Results of step load increase and decrease

5. CONCLUSION

This paper describes the dynamic modelling of PEM Fuel Cells, which can be used in different dynamic studies especially in vehicle applications. The obtained results showed a good agreement between the steady-state performance of the model and the datasheet provided by the manufacture. In addition, the dynamic performance showed fast response to load variations. The PI controller succeeded to regulate the unit performance regarding the output voltage. Thus, it is possible to obtain a regulated performance from the unit even with load variations. This study enables the prediction of PEMFC dynamic behaviour under different operating conditions, which lays down a foundation for optimization and control development that can be used with electric vehicles.
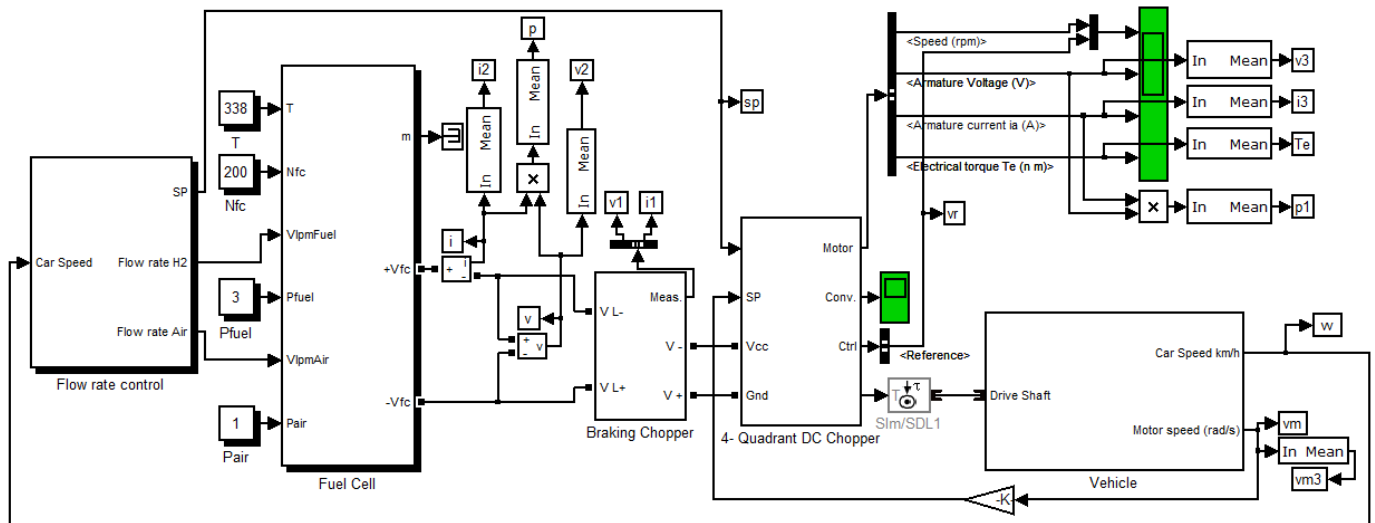
Fig. 10. Fuel-cell-based electric vehicle model

6. REFERENCES

[1] J.J. Baschuk, Xianguo Li, "A general formulation for a mathematical PEM fuel cell model", Journal of Power Sources, 142 (2004), pp. 134–153

[2] E. Andrea, M. Ma˜nana, A. Ortiz, C. Renedo, L.I. Egu´ıluz, S. P´erez, F. Delgado, "A simplified electrical model of small PEM fuel cell", E.T.S.I.I.T. University of Cantabria.

[3] R.Seyezhai, B.L.Mathur, "Mathematical Modeling of Proton Exchange Membrane Fuel Cell", International Journal of Computer Applications (0975 – 8887) Volume 20– No.5, April 2011.

[4] Mikko Mikkola, "Experimental Studies on Polymer Electrolyte Membrane Fuel Cell Stacks", Helsinki University of technology, 2001

[5] M.Y. El-Sharkh, A. Rahman, M.S. Alam, P.C. Byrne, A.A. Sakla, T. Thomas, "A dynamic model for a stand-alone PEM fuel cell power plant for residential applications", Journal of Power Sources 138 (2004) 199–204

[6] M. Meiler, O. Schmid, M. Schudy, E.P. Hofer, "Dynamic fuel cell stack model for real-time simulation based on system identification", Journal of Power Sources 176 (2008) 523–528.

[7] P.R. Pathapati, X. Xue, J. Tang, "A new dynamic model for predicting transient phenomena in a PEM fuel cell system", Renewable Energy, Vol. 30, Issue 1, January 2005, Pages 1–22

[8] C. Panos, K.I.Kouramas, M.C.Georgiadis, E. N. Pistikopoulos, "Modelling and explicit model predictive control for PEM fuel cell systems", Chemical Engineering Science (January 2012), 67 (1), pp: 15-25

[9] A. Rowe and X. Li, "Mathematical modeling of proton exchange membrane fuel cells", J. Power Sources, vol. 102, no. 1–2, pp. 82–96, Dec. 2001

[10] J. Alejandro, A. Arce, C. Bordons, "Development and experimental validation of a PEM fuel cell dynamic model", Journal of Power Sources, Volume 173, Issue 1, 8 November 2007, Pages 310-324

[11] S.M Sharifi, S. Rowshan Zamir, M.H. Eikani, "Modelling and simulation of the steady-state and dynamic behaviour of a PEM fuel cell", Energy 35 (2010), Vol. 35, Issue 4, pp: 1633-1646

[12] S. Pasricha, R. Steven Shaw, "A Dynamic PEM Fuel Cell Model", IEEE Transactions on Energy Conversion, Vol. 21, No. 2, June 2006

[13] S. Busquet, C.E. Hubert, J. Labbé, D. Mayer, R. Metkemeijer, "A new approach to empirical electrical modelling of a fuel cell, an electrolyser or a regenerative fuel cell", Journal of Power Sources, Vol. 134, pp. 41–48, 2004

[14] NedStack PS6 Product Data, Ned Stack fuel cell technology,http://www.fuelcellmarkets.com/content/images/articles/ps6.pdf

[15] C. Wang, M. H. Nehrir, "Dynamic Models and Model Validation for PEM Fuel Cells Using Electrical Circuits, Energy Conversion", IEEE Transactions on, Vol.20, No.2, June 2005, pp. 442-451

[16] Peng Quan, "A study of PEM fuel cell modelling", Thesis of Master of Engineering, Ryerson University, 2003.

[17] Andres Gabriel Christou, "Hydrogen Fuel Cell Power System Performance of Plug Power Gen Core 5B48 Unit", thesis of Master of science, University of Strathclyde Engineering, 2010

[18] W. E. Wasburn, "International Critical Tables of Numerical Data", Physics, Chemistry and Technology, 1ˢᵗ Electronic Edition, Knovel: Norwich, NY, (2003)

[19] C. Spiegel, "PEM Fuel Cell Modelling and Simulation Using MATLAB", Elsevier Academic Press, Oxford UK, 2008

[20] LI Wei, ZHU Xin-jian, CAO Guang-yi, "Modeling and control of a small solar fuel cell hybrid energy system", Journal of Zhejiang University SCIENCE A, 2007 8(5):734-740.

[21] Song-Yul Choe, Jong-Woo Ahn, Jung-Gi Lee, Soo-Hyun Baek, "Dynamic Simulator for a PEM Fuel Cell System with a PWM DC/DC Converter", IEEE Transactions on Energy Conversion, Vol. 23, No. 2, June 2008

[22] www.mathworks.com, 2010.

[23] R.F. Mann, J.C. Amphlett, B.A. Peppley, C.P. Thurgood, "Application of Butler–volmer equations in the modelling of activation polarization for PEM fuel cells", Journal of Power Sources 161 (2006), pp. 775–781

[24] R.F. Mann, J.C. Amphlett, B.A. Peppley, C.P. Thurgood, "Henry's Law and the solubilities of reactant gases in the modelling of PEM fuel cells", Journal of Power Sources 161 (2006) pp. 768–774